Mineral Wool Production Monitoring Using Neural Networks

Marko Hočevar, Brane Širok, and Bogdan Blagojević

University of Ljubljana,
Faculty of mechanical engineering,
Aškerčeva 6, SI-1000 Ljubljana, Slovenia

marko.hocevar@fs.uni-lj.si, brane.sirok@fs.uni-lj.si, bogdan.blagojevic@fs.uni-lj.si

Abstract

Homogeneity of the primary layer in mineral wool production process is required for high quality products. State-of-the-art measurement techniques for the evaluation of primary layer homogeneity are very slow and can only be applied after the product is manufactured. We present here a method that enables on-line monitoring and control and is based on experimental modeling using neural networks. The experimental method is based on image acquisition and image processing of the mineral wool primary layer structure. As a estimator of the mineral wool primary layer structure and quality, the weight of the primary wool layer is used, measured by an on - line weighting device in four locations of the conveyor belt. The instrumentation of on - line weighting device was upgraded for the purpose of the present experiment and enabled high speed acquisition of all measurement channels. The structure of the mineral wool primary layer was measured by visualization of the modified entrance to the on - line balance using a CCD camera. All data channels were simultaneously sampled. Radial basis neural networks are used for prediction. The structure of the mineral wool primary layer is predicted on the basis of experimentally provided weights data. The learning set consists of weights - images pairs. The prediction of the mineral wool primary layer structure consists of providing only weights. A good agreement between statistical properties of measured and modeled structures of the primary wool layer like spatial homogeneity of the primary mineral wool layer thickness, is shown. The results of the study confirm that the time - delayed vector of weights bears enough information for the monitoring of the production process. The modeling of primary mineral wool structure is of lesser quality due to high dimensionality of the modeled variable.
Keyword: mineral wool, radial basis neural networks, prediction, visualization.

I. Introduction

Homogeneity of the primary layer in mineral wool production processes is required for high quality products. State-of-the-art measurement techniques for the evaluation of primary layer homogeneity are very slow. Our goal was to solve the following problem: *how can the homogeneity of the mineral wool primary layer and speed of the secondary conveyor belt be modeled based on the measurement data provided by four measurement cells on the primary layer balance?* This novel method once fully developed will enable on-line monitoring and control. The method is based on experimental prediction using neural networks with training data provided from computer-aided visualization and weighting of the primary layer.

Mineral wool is a general name for many inorganic insulation materials made of fibers. Mineral wool is usually divided into different subgroups, depending on the raw materials from which they are made, such as rock wool, glass wool, and slag wool. The most frequently used raw materials for mineral wool production are diabase, dolomite, granite, basalt, limestone, etc. Because of its amorphous structure, mineral wool has excellent sound and thermal insulation properties. There are several production methods for mineral-wool fibers, with a wide variation of quality and quantity of the final product [1]. The most commonly used mineral wool production process is the fiberisation process of molten rock on rapidly rotating spinning discs [2–4]. Molten rock enters through a siphon neck in a homogenization reservoir. Over a weir and a directing channel, the molten rock falls under gravity onto a rotating disc of the spinning machine. The schematic of the production process from the beginning to the end of the primary layer production is shown in Fig. 1. After this the mineral wool enters the conveyor belt of the secondary mineral wool layer where it is thermally treated and finalized to selected density, thickness and size. The speed of secondary conveyor belt should be regulated according to the measurements on the primary layer balance to ensure the proper thickness and density of the final product. The speed of the secondary conveyor belt is many times lower than the speed of the primary conveyor belt as the secondary layer is composed of up to 50 primary wool layers, depending on the type of the final product. The complete production line is about 60 meters long.

The fall of molten rock onto the spinning discs and the formation of a thin layer of melt on the discs on which the mineral wool fibers are formed is presented in Fig. 2. Formed fibers enter into a coaxial blow-away flow, which spreads around the circumference of the spinning discs. The coaxial air flow transports the mineral wool fibers into a wool chamber where they solidify into fibers which have a diameter of about 5 μm and a length of approximately 10mm. Besides the basic blow-away flow that transports the fibers in the region of a moving perforated mesh, a secondary suction air flow is formed in the wool chamber which ensures the negative pressure in the chamber, and the air flow direction onto the perforated mesh. That consequently, causes the subsiding of the mineral wool fibers on the mesh and the formation of the primary layer.

The formation mechanism, as mentioned in Ref. [4], is described by Eisenklam [5]. Fiber is formed from a molten film on spinning discs. The formation and motion of the fiber depends on the inertial, viscous, and surface tension forces. The solidification process depends on the thermodynamic and mass properties of the melt. In Ref. [4], a model is presented which describes the breaking mechanism and formation of mineral fibers with a spinning machine. The temperature, position, and internal tension of a single fiber during the formation phase are calculated according to the effects of the inertial and aerodynamic forces. The quality of the final product, on a microscale, depends on the structure of fibers and the proportion of solidified pellets in the mineral wool. The fiber structure is characterized by its thickness (diameter), its length, and the variation of both respective quantities. The material that is not transformed into fibers remains in the form of solidified shots, which arise from an incomplete fiberisation process [2,3].

Two primary layer sample images are shown in Fig. 4 and Fig. 5, corresponding to the production line parameters denoted as ‘‘good’’ (Fig. 4) and ‘‘bad’’ (Fig. 5), respectively. The example shows significant influence of production line parameters on the structure and quality of the primary layer.

In the following sections of the article some basic characteristics of experimental set-up and experimental modeling are explained. The performance of the method is then estimated by comparing the properties of the estimated data with the corresponding measured data.

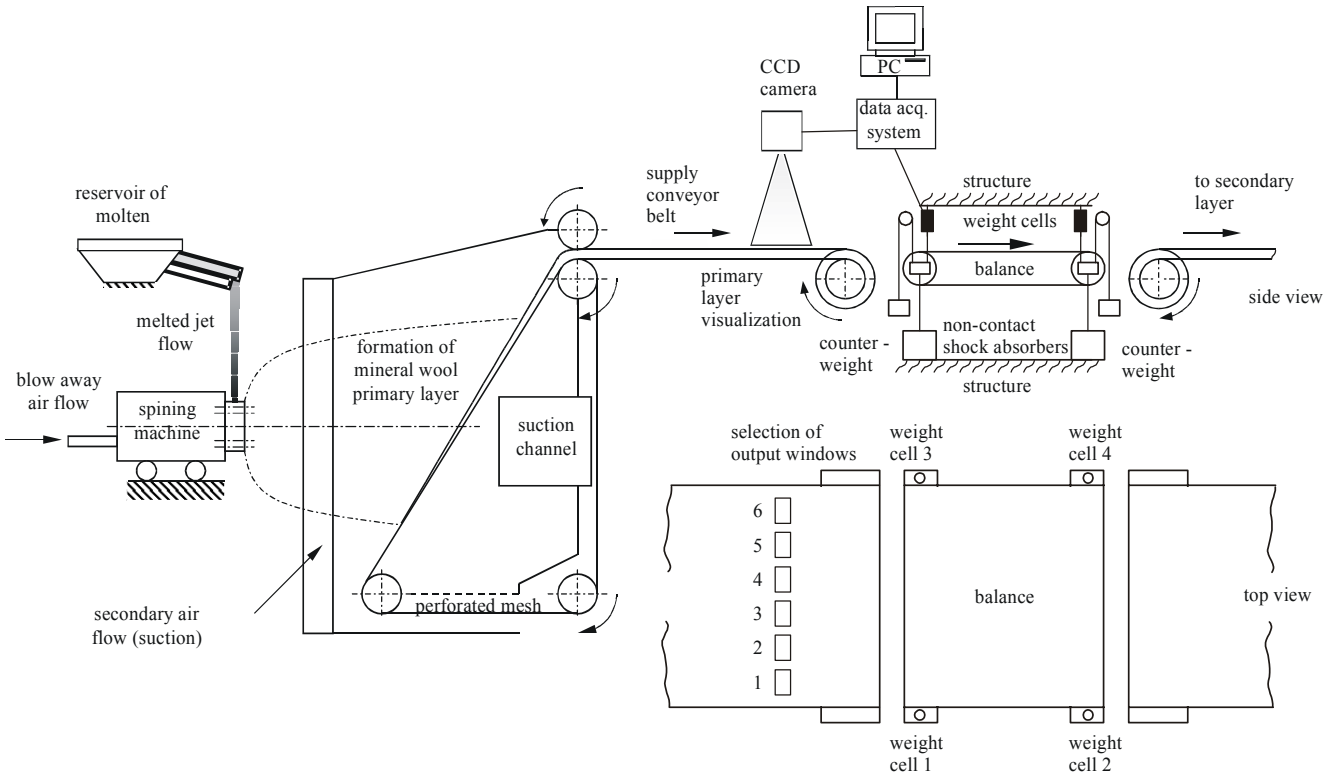

Fig. 1. Schematics of the primary layer part of the production line.

.

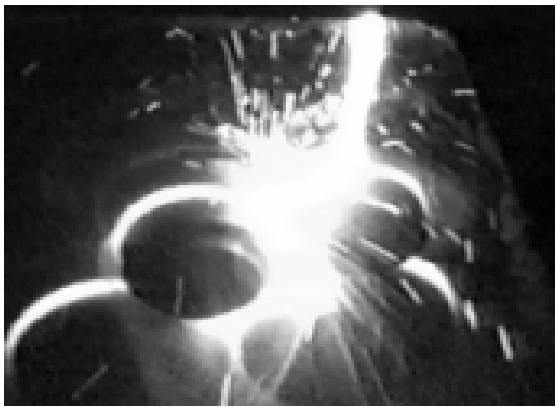

Fig. 2. Fiberisation process on a machine.

Fig. 3. Sample of mineral wool fibres.

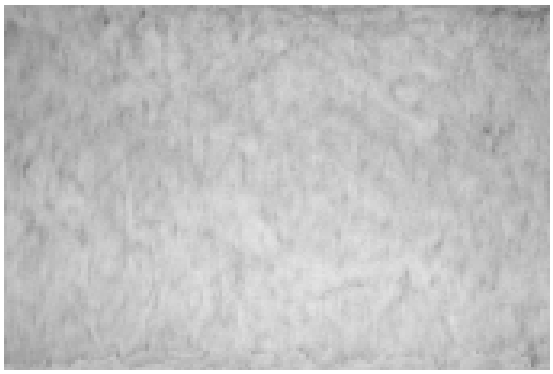

Fig. 4. Homogeneous structure of primary wool layer.

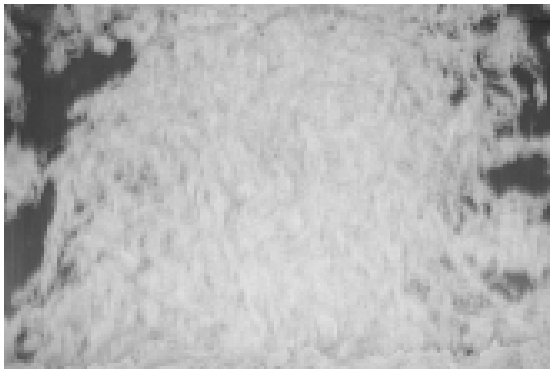

Fig. 5. Non-homogeneous structure of primary wool layer.

II. Experimental set-up

The balance for the measurement is normally used for the measurements of mean weight of the primary wool layer as shown in Fig. 1. The specific weight of the primary layer during normal operation is from 30 to 100 g/m^2, while during the present experiment it was set to 80 g/m^2. The dimensions of the balance are approximately 1.5x2.5 m and the structure is due to its heavy weight balanced by counterweights. The system is equipped with large non-contact shock absorbers to reduce high frequency vibrations. The balance was carefully cleaned, serviced and calibrated prior to the experiment to reduce the structural vibration to a minimum. The measurement uncertainty of the balance, which is during normal operation about 40 g, was reduced for the time of the present experiment and was less than 20 g which equals 7%. The speed of the primary layer conveyor belt was set to 1m/s.

Measurement of weight was performed by four 5 kg load measurement cells from Hottinger Baldwin Messtechnik type Z6. The power to the load cells was supplied by a precise current supply from the corresponding measurement amplifier of the same producer. Signal was measured in the position of the balance with the SCXI 1120 module from national Instruments, amplified and filtered by a low pass filter with cut off frequency 10 kHz. The data acquisition was performed by a National instruments AT-MIO-16E-10 board. The sampling frequency was 10000Hz, but was later for the purpose of better modeling down sampled to 500 Hz as explained in section 4.

Visualization was performed on the supply conveyor belt 1 m before the balance. The production line was modified for the present experiment to enable the installation of the camera in the selected position. The structure of the balance unfortunately prevents the visualization of the primary layer on the balance. The measurements were performed by a CCD camera Sony XC-HR50, connected to a National Instruments Type 1409 frame grabber. The resolution of images was 640x480 pixels at a

frame rate 25/s. The camera position and illumination were selected as shown in Fig. 1, and did not change during the experiment. The illumination was provided by a single photographic light. The synchronization between the weight and image was performed over PC internal synchronization bus of the both data acquisition and framegrabber board.
Four different measurement points were selected according to the different values of blow-away air volume flow and rotational speed of the rotating disks.
Analysis is performed on every image in a sequence in six selected windows, arranged as shown in Fig. 1. For every image in the sequence, an average intensity $A(k, t)$ in each window is calculated as

$$A(k,t) = \sum_{l} \sum_{m} E(l,m) \quad . \tag{1}$$

Here, k denotes the successive window number in each frame and t denotes the successive acquired images; the intensity of pixels, $E(l, m)$, ranges from 0 to 255, corresponding to the 8-bit resolution of the camera; l and m are the coordinates of the pixels inside the window (k, t). The A values where the primary layer is non-homogeneous and interrupted are lower, since the background is darker than the mineral wool. The average intensity of the windows is not calibrated to the weight of the mineral wool primary layer, but we estimate that a functional relationship between both variables exists. The size of each input window is approximately 0.2x0.3 m.

III. Modeling with radial basis function neural networks (RBFNN)

A natural law is usually described by the relationship between dependent and independent variables $y = f(\mathbf{x})$. In our case $\mathbf{x}$ represents the independent data vector of the weights, while y describes the dependent data of grey level intensities in the selected output region. The fundamental problem is to formulate a method by which the function f can be estimated based on given experimental data. We proceed with a non-parametric estimation by means of the RBFNN, which learns to estimate the function f from the provided measured samples [6]. RBFNNs might require more neurons than standard, feed-forward, back-propagation networks, but often they can be designed in a fraction of the time necessary to train a standard feed-forward network.
The RBFNN is an information-processing system consisting of K memory cells called neurons with a localized receptive field. This field is described by a radially symmetric basis function $g(\mathbf{x})$ of the input vector $\mathbf{x}$. We employ the Gaussian function, $g_k(\mathbf{x})$

$$g_k(\mathbf{x}) = \exp\left(-\frac{\left\| \mathbf{x} - \mathbf{q}_k \right\|^2}{2\sigma_k^2} \right) , \tag{2}$$

in which the parameters $\mathbf{q}_k$ and σ_k denote the center and the width, respectively, of the receptive field of the k-th neuron. All the neurons obtain the same input $\mathbf{x}$. The output $y(\mathbf{x})$ from the network is described by a linear superposition of the individual outputs

$$y(\mathbf{x}) = \sum_{k}^{K} m_k g_k(\mathbf{x}) \quad . \tag{3}$$

This superposition represents the model of function f, which is specified by the set of parameters, m_k, q_k and σ_k. They are statistically estimated from a given set of experimental samples ($\mathbf{x}_n$,y_n), $n = 1 \ldots N$, such that the mean-square error between the network output $y(\mathbf{x}_n)$ and experimental data is a minimum. Various algorithms are available for minimizing the mean-square error. We use an algorithm based on the orthogonal least squares method according Chen et al [7]. Orthogonal least squares is a forward selection procedure based on the classical Gram-Schmidt orthogonalization

procedure. The number of neurons, K, is set by the algorithm, so that the addition of new neurons does not reduce the criterion function by more than the selected value.
The estimation using neural networks depends on the parameters of the model. The number of neurons K; the centers of the neurons $\mathbf{q}_k$; the spread σ_k; the weight m_k; and the length j of the input is adjusted by the model for each operation point.
The size of the learning set is limited to N=2000 ($\mathbf{x}$, y) input-output pairs. The behavior of the model is tested on the modeling set including 1000 sample pairs. The parameters derived by learning set are used for modeling set. The system is trained anew for each measurement point.
Prior to the modeling, the input data are normalized to a zero mean value and a standard deviation of 1.

IV. Results and discussion

A result of the modeling average window intensity in the window 1 of the measurement point 3 is shown in figure 6. The overall modeling performance of average window intensities is acceptable with the regression coefficient (between the measured and modeled average window intensities in measurement point 3), r=0.73. Very similar results are found also in other measurement points, the regression coefficient is from r=0.62 to r=0.77. In general slightly better agreement is achieved in the measurement points where the fluctuations of the average window intensity are smaller.
The influence of the length of the input j is presented in figure 7. The maximum agreement is around the 0.25 seconds or 0.25 m, which is close to the size of the input window, whose size in the direction of the conveyor belt is approximately 0.2 m. The sampling rate of the weights measurements is 10000 Hz, which proved to be too high due to the efficiency of the installed non-contact shock absorbers. Use of the very long weights input data caused additional modeling error. To correct this, the weights input data are down sampled by a factor of 20. Using this, the maximum agreement is achieved, but no in depth analysis is performed and modeling errors are not evaluated for other down sampling factors.
We believe that the very high dimensionality of the visualization data and corresponding lower dimensionality of the weights data are the main reasons for the poor performance of average window intensity modeling. It is known that if the dimension of the network input is comparable to the size of the training set, the system is liable to overfitting and the result will be poor generalization [8], which is also the case in this work. A data-reduction method like principal component analysis could possibly be applied to overcome these problems. By reducing the input-vector dimensionality, a shorter calculation time required for the estimation could be achieved; and this could also render an online estimation of the flow properties possible. For the monitoring however, only the statistical properties, averaged over certain time interval, are required. Rapid changes of the mineral wool production process are also not possible.

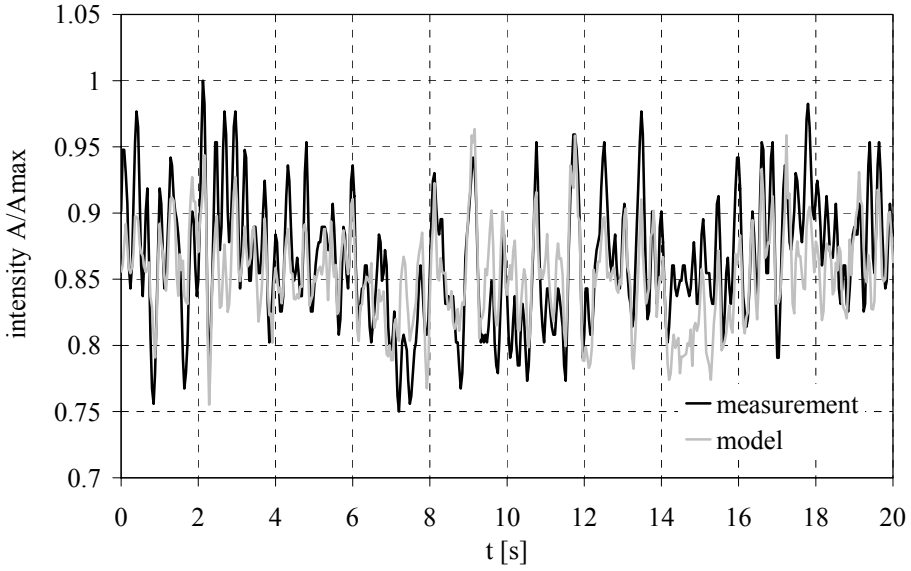

Fig. 6. The measured and modeled average window intensities, measurement point 3, window 1.

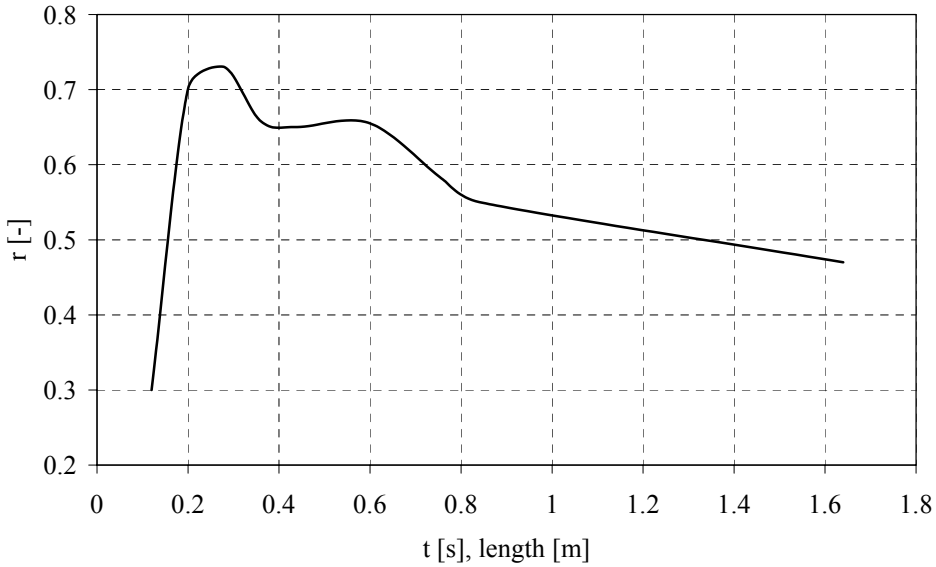

Fig. 7. The influence of the length of the input *j* on the correlation coefficient between the measured and modeled average window intensities, measurement point 3, window 1.

The modeling procedure using neural networks is proved to be valuable in this particular problem where the functional relationship between independent and dependent variables is not known. It offers the possibility that other parameters may be included in the modeling procedure also in the future. The use of the radial basis function neural networks is proved to be satisfactory, however comparison with other methods prior to the installation of the system for permanent monitoring must be performed. The performance of a RBF neural network critically depends on the chosen centers. The original RBF method requires that there are as many RBF centers as there are data points. Based on a large number of data samples, the structure of the RBF neural network is usually complex. Furthermore, numerical ill conditioning frequently occurs owing to the near-linear dependency caused by some centers being too close [9]. For the minimizing of the mean-square error the orthogonal least squares method is selected. Orthogonal least squares is a forward selection procedure based on the classical Gram-Schmidt orthogonalization procedure. The orthogonal least-squares method is used to choose radial basis function centers one by one until an adequate network

has been constructed. Another common learning algorithm for radial basis function networks is based on first randomly choosing some data points as radial basis function centers and then using a singular-value decomposition to solve for the weights of the network. Such a procedure has several drawbacks [7, 10] and, in particular, the arbitrary selection of centers is unsatisfactory. No special attention is paid to reduce the time required for learning.
Further improvements should be carried out regarding the measurement procedure. The balance is due to the large size and weight influenced by low frequency structural vibrations, which increase during long-time operation due to deposition of dirt. Although this problem was treated with utmost care, structural vibration could not be fully eliminated. For detection of non-homogeneity the installation of the camera could be adequate, but the space in the production process without modifications is very limited, the environmental condition do not favor permanent camera installation in the close vicinity of the production chamber, and the regulation of the speed of the secondary conveyor belt using only camera is not possible.

Table 1. Comparison of the parameters of the measured and modeled data.

measurement point	window	average value	standard deviation	average value	standard deviation	regression value
		measurement		model		
1	1	0.804	0.069	0.821	0.077	0.685
2	1	0.839	0.060	0.837	0.053	0.623
3	1	0.855	0.048	0.844	0.039	0.73
4	1	0.880	0.043	0.827	0.048	0.769

V. Conclusions

The presented method proves to be promising for the control of the mineral wool production process. The future work should be aimed towards optimizing the number and dimensionality of samples used in the modeling, improvement of the measurement method, neural network modeling algorithm and calibration of the window average intensity, i.e. relation with average weight of the primary wool layer.
However experiential work on the process line is difficult, very expensive, and has thus to be agreed in advance with the operator of the plant.

References

[1] Ohberg, I., Technological development of the mineral wool industry in Europe, Ann. Occup. Hyg. 1987, 31, (4B), 529–545.
[2] Trdic, F., Sirok, B., Bullen, P.R., Philpott, D.R., Real time imaging, 1999, 5, (2), 125–140.
[3] Angwafo, A.W., Bullen, P.R., Philpott, D.R., Melt flow in the production of mineral wool by centrifugal spinning, Proc. FEDSM'98, 1998 ASME Fluids Eng. Div. Summer Meeting, Washington, USA, June 21–25, 1998.
[4] Westerlund, T., Hoikka, T., On the modeling of mineral fiber formation, Comput. Chem. Eng. 1989, 13 (10), 1153–1163.
[5] Eisenklam, P., On ligament formation from spinning discs and cups, Chem. Eng. Sci., 1964, 19, 693–694.
[6] Grabec, I., Sachse, W., Synergetics of Measurement, Prediction and Control, 1997, Springer, Berlin.
[7] Chen, S., Cowan, C.F.N., and Grant, P. M., Orthogonal Least Squares Learning Algorithm for Radial Basis Function Networks, IEEE Trans. Neural Networks, 1991, 2, (2), 302-309.

[8] Yuan J. L., Fine, T. L., Neural-Network design for small training sets of high dimension, IEEE Trans. Neural Networks, 1998, 9, (2), 266–280.
[9] Han, M., Xi, J., Efficient clustering of radial basis perceptron neural network for pattern recognition, Pattern Recognition, 2004, 37, (10), 2059– 2067.
[10] Gomm, J.B., Yu, D.L., Selecting radial basis function network centers with recursive orthogonal least squares training, IEEE Trans. Neural Networks, 2000, 11, (2), 306–314.

Marko Hočevar was born in Ljubljana, Slovenia in 1972. He obtained his degree in physics in 1997 and PhD 2003. He is currently an assistant at University of Ljubljana, Faculty of mechanical engineering. His research interests include non-parametric modeling of various non-linear processes by neural networks and measurements in the field of turbomachinery.

Brane Širok was born in Ljubljana, Slovenia in 1952. He received his degree in 1980, and PhD in 1990 in mechanical engineering. From 1996 he is a professor at the department for hydraulic machinery at University of Ljubljana. His main research areas are turbomachinery design and application, experimental analysis of non-linear chaotic phenomena in fluid dynamics, including computer-aided visualization techniques.

Bogdan Blagojević was born in Slovenj Gradec, Slovenia in 1963. He obtained his degree in mechanical engineering in 1988 and PhD 1996. His main research interest is development of multi-regression experimental methods of industrial processes.